Structural Engineering and Mechanics, Vol. 16, No. 2 (2003) 153-176

DOI: http://dx.doi.org/10.12989/sem.2003.16.2.153

The exact solutions for the natural frequencies and mode shapes of non-uniform beams carrying multiple various concentrated elements

Der-Wei Chen†

Department of Naval Architecture and Marine Engineering, Chung Cheng Institute of Technology, National Defense University, Yuansulin, Dashi, Taoyuan, Taiwan 335, Republic of China

(Received October 23, 2002, Revised March 31, 2003, Accepted May 26, 2003)

Abstract. From the equation of motion of a “bare” non-uniform beam (without any concentrated elements), an eigenfunction in term of four unknown integration constants can be obtained. When the last eigenfunction is substituted into the three compatible equations, one force-equilibrium equation, one governing equation for each attaching point of the concentrated element, and the boundary equations for the two ends of the beam, a matrix equation of the form $[B]\{C\} = \{0\}$ is obtained. The solution of $|B| = 0$ (where $|\cdot|$ denotes a determinant) will give the “exact” natural frequencies of the “constrained” beam (carrying any number of point masses or/and concentrated springs) and the substitution of each corresponding values of $\{C\}$ into the associated eigenfunction for each attaching point will determine the corresponding mode shapes. Since the order of $[B]$ is $4n + 4$, where n is the total number of point masses and concentrated springs, the “explicit” mathematical expression for the existing approach becomes lengthily intractable if $n > 2$. The “numerical assembly method”(NAM) introduced in this paper aims at improving the last drawback of the existing approach. The “exact” solutions in this paper refer to the numerical results obtained from the “continuum” models for the classical analytical approaches rather than from the “discretized” ones for the conventional finite element methods.

Key words: non-uniform beam; natural frequencies; mode shapes; bare beam; constrained beam; eigen-function.

1. Introduction

The free vibration problem for a “uniform” beam carrying various concentrated elements, has been studied by many researchers (Laura *et al*. 1975, 1977, 1987, Gurgoze 1984, Wu and Lin 1990, Hamdan and Jubran 1991, Rossi *et al*. 1993, Gurgoze 1998, Wu and Chou 1998, Wu and Chen 2001). Sankaran *et al*. (1975), Lee (1976), De Rosa and Auciello (1996), Wu and Chou (1999), Qiao *et al*. (2002), Li (2002) are the few studies concerned about the free vibration analysis of the “uniform” and “non-uniform” beams carrying concentrated elements. In this paper, the numerical assembly method (NAM) presented in Wu and Chen (2001) and Wu and Chou (1999) for the free vibration analysis of a “uniform” beam carrying multiple sprung masses was used to tackle the title problem. One of major differences between (Qiao *et al*. 2002, Li 2002) and the present paper is that the beams studied are “stepped” in the former and “tapered” in the latter. Since a stepped beam is

† Associate Professor

considered as a combination of multiple “uniform beam segments” with different cross-sectional areas in Qiao *et al.* (2002), Li (2002) and this is not true for a tapered beam in this paper, the mode shape functions for the “stepped” beams presented in Qiao *et al.* (2002), Li (2002) are not suitable for the “tapered” beams studied in this paper.

From the following sections of this paper, one finds that the eigen equation of the title problem takes the form $[B]\{C\} = \{0\}$. Since the order of the overall coefficient matrix $[B]$ is $p = 4n + 4$, with n being the total number of concentrated attachments, the order of $[B]$ is 8 for one attachment and 12 for two attachments. It is evident that the explicit expression for the eigen equation $[B]\{C\} = \{0\}$ will become lengthy and complicated for the cases with $n > 2$, hence the literature relating to the free vibration analysis of a non-uniform beam carrying more than “two” concentrated attachments is rare. Because the numerical assembly method (NAM) presented in Wu and Chen (2001) and Wu and Chou (1999) has been found to be able to easily tackle the free vibration problem of a “uniform” beam carrying any number of concentrated attachments, this paper tries to use the same approach to perform the free vibration analysis of the constrained “non-uniform” (tapered) beams studied in this paper. The key point of the NAM is as follows: If the “left” side and the “right” side of each attaching point together with the “left” end and the “right” end of the non-uniform beam are considered as the nodal points, and the associated integration constants, C_{vi} ($v = 1$~n; $i = 1$~4), are considered as nodal displacements, then the associated coefficient matrix, $[B_L]$, $[B_v]$ ($v = 1$~n) or $[B_R]$, may be considered as the element stiffness matrix of a beam element, so that the conventional assembly technique of the direct stiffness matrix method for the finite element method (FEM) (Bathe and Wilson 1976) may be used to obtain the “overall” coefficient matrix $[B]$. Any trial value of $\bar{\omega}_j$ that renders the value of the determinant $|B|$ vanishes denotes one of the eigenvalues of the “constrained” non-uniform beam (carrying multiple concentrated elements).

To show the reliability of the introduced approach, the lowest five natural frequencies and some of the corresponding mode shapes of a doubly-tapered beam carrying five concentrated elements were calculated. Six boundary conditions were studied: free-clamped, clamped-free, simply supported - clamped, clamped-simply supported, clamped-clamped, and simply supported-simply supported. It has been found that the agreement between the present results and the FEM results is good.

For convenience, the non-uniform beam with prescribed boundary conditions is called the “unconstrained” (or “bare”) beam if it carries no attachment and is called the “constrained” beam if it carries any attachments.

2. Eigenfunctions of the constrained non-uniform beam

Fig. 1 shows a cantilevered doubly-tapered beam carrying n concentrated elements. The whole cantilevered non-uniform beam with length L is subdivided into $(n + 1)$ segments by the attaching point v located at $x = x_v$ (v = 1, 2, ..., n), where denotes the v-th “attaching point” and ( ) denotes the v-th “beam segment”. In addition, the “left” end and the “right” end of the beam are denoted by L and R, respectively.

The equation of motion for a “bare” non-uniform beam is given by De Rosa and Auciello (1996), Gorman (1975)

$$\frac{\partial^2}{\partial x^2}\left[EI(x)\frac{\partial^2 y(x,t)}{\partial x^2}\right] + \rho A(x)\frac{\partial^2 y(x,t)}{\partial t^2} = 0 \tag{1}$$

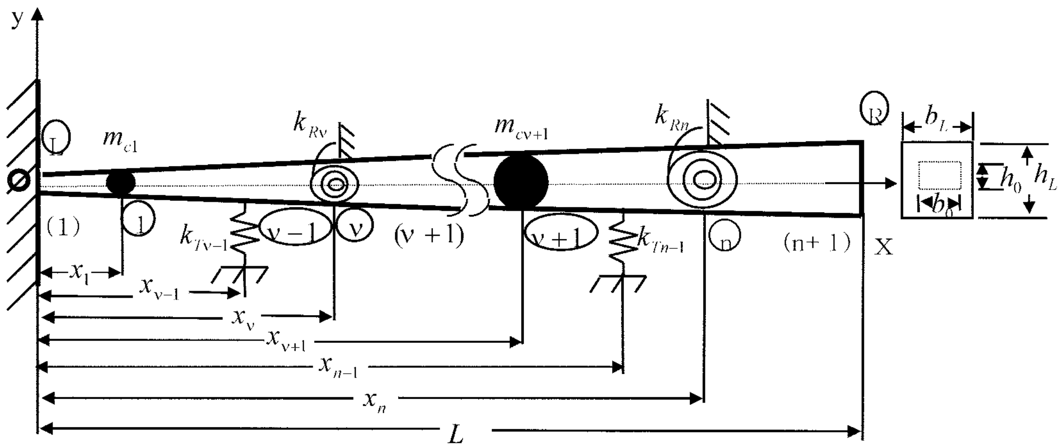

Fig. 1 A cantilevered doubly-tapered beam carrying n concentrated elements

where $y(x, t)$ is the transverse deflection, E is the Young's modulus, $A(x)$ is the cross-sectional area at the position x, $I(x)$ is the moment of inertia of $A(x)$, ρ is the mass density of the beam material and t is time.

For the doubly-tapered beam as shown in Fig. 1, the cross-sectional area $A(x)$ and its moment of inertia $I(x)$ take the forms

$$A(x) = A_0\left[(\alpha - 1)\frac{x}{L} + 1\right]^2, \tag{2a}$$

$$I(x) = I_0\left[(\alpha - 1)\frac{x}{L} + 1\right]^4 \tag{2b}$$

where $A_0 = b_0 h_0$ and $I_0 = b_0 h_0^3/12$ are the cross-sectional area and moment of inertia of the cross-section of the tapered beam with width b_0 and height h_0 at $x = 0$ (see Fig. 1), respectively, while $\alpha = h_L/h_0 = b_L/b_0$ is the taper ratio of the beam with width b_L and height h_L at $x = L$. It is noted that $A(x)$ and $I(x)$ are the two key parameters for a non-uniform beam, because they affect the magnitudes of the sectional mass ($\rho A(x)$) and sectional stiffness ($EI(x)$) of the non-uniform beam as one may see from Eq. (1).

For free vibration of the beam, one has

$$y(x, t) = \bar{Y}(x)e^{i\bar{\omega}t} \tag{3}$$

where $\bar{\omega}$ is the natural frequency of the "constrained" beam and $\bar{Y}(x)$ is the amplitude of $y(x, t)$.

The substitution of Eqs. (2) and (3) into Eq. (1) yields

$$\left[(\alpha - 1)\frac{x}{L} + 1\right]^4 \frac{d^4\bar{Y}(x)}{dx^4} + 8\left[(\alpha - 1)\frac{x}{L} + 1\right]^3 \left(\frac{\alpha - 1}{L}\right) \frac{d^3\bar{Y}(x)}{dx^3}$$

$$+ 12\left[(\alpha - 1)\frac{x}{L} + 1\right]^2 \left(\frac{\alpha - 1}{L}\right)^2 \frac{d^2\bar{Y}(x)}{dx^2} - \frac{\rho A_0 \bar{\omega}^2}{EI_0}\left[(\alpha - 1)\frac{x}{L} + 1\right]^2 \bar{Y}(x) = 0 \tag{4}$$

If the following non-dimensional parameter was introduced

$$\xi(x) = (\alpha - 1)\frac{x}{L} + 1 \tag{5}$$

then Eq. (4) reduced to

$$\xi^4 Y''''(\xi) + 8\xi^3 Y'''(\xi) + 12\xi^2 Y''(\xi) - \xi^2\left[\frac{L\Omega}{(\alpha - 1)}\right]^4 Y(\xi) = 0 \tag{6a}$$

where a prime denotes the derivative with respect to ξ and

$$(\Omega L)^4 = \frac{\rho A_0 \bar{\omega}^2 L^4}{EI_0} \tag{6b}$$

The general solution of Eq. (6a) takes the form De Rosa and Auciello (1996), Gorman (1975), Karman and Biot (1940)

$$\bar{Y}(\xi) = \xi^{-1}[C_1 J_2(\beta\sqrt{\xi}) + C_2 Y_2(\beta\sqrt{\xi}) + C_3 I_2(\beta\sqrt{\xi}) + C_4 K_2(\beta\sqrt{\xi})] \tag{7}$$

where $C_i (i = 1\sim4)$ are the integration constants, $\beta = 2L\Omega/(\alpha - 1)$, J_2 and Y_2 are the second order Bessel functions of first kind and second kind, while I_2 and K_2 are the second order modified Bessel functions of first kind and second kind.

Eq. (7) represents the eigenfunction for the transverse deflection of the constrained beam. Once the natural frequencies $\bar{\omega}_j$ (j = 1, 2, ...) and the constants for each attaching point, C_i (i = 1~4), are determined from the next sections, one may obtain the value of $\bar{Y}_j(\xi)$. The latter are the mode shapes of the constrained beam corresponding to the natural frequency $\bar{\omega}_j$.

For "the v-th beam segment", from Eq. (7) one has

$$\bar{Y}_v(\xi_v) = \xi_v^{-1}[C_{v1} J_2(\beta\sqrt{\xi_v}) + C_{v2} Y_2(\beta\sqrt{\xi_v}) + C_{v3} I_2(\beta\sqrt{\xi_v}) + C_{v4} K_2(\beta\sqrt{\xi_v})] \tag{8}$$

with

$$\xi_v = (\alpha - 1)\frac{x_v}{L} + 1 \tag{9}$$

The differentiation of $\bar{Y}_v(\xi_v)$ with respect to ξ_v gives

$$\bar{Y}'_v(\xi_v) = -\frac{\beta}{2}\xi_v^{-3/2}[C_{v1} J_3(\beta\sqrt{\xi_v}) + C_{v2} Y_3(\beta\sqrt{\xi_v}) - C_{v3} I_3(\beta\sqrt{\xi_v}) + C_{v4} K_3(\beta\sqrt{\xi_v})] \tag{10}$$

$$\bar{Y}''_v(\xi_v) = \left[\frac{\beta}{2}\right]^2 \xi_v^{-2}[C_{v1} J_4(\beta\sqrt{\xi_v}) + C_{v2} Y_4(\beta\sqrt{\xi_v}) + C_{v3} I_4(\beta\sqrt{\xi_v}) + C_{v4} K_4(\beta\sqrt{\xi_v})] \tag{11}$$

$$\bar{Y}'''_v(\xi_v) = -\left[\frac{\beta}{2}\right]^3 \xi_v^{-5/2}[C_{v1} J_5(\beta\sqrt{\xi_v}) + C_{v2} Y_5(\beta\sqrt{\xi_v}) - C_{v3} I_5(\beta\sqrt{\xi_v}) + C_{v4} K_5(\beta\sqrt{\xi_v})] \tag{12}$$

where J_n and Y_n are the n-th order Bessel functions of first kind and second kind, while I_n and K_n are the n-th order modified Bessel functions of first kind and second kind with n = 3, 4, 5.

3. Coefficient matrix [B_v] for the v-th attaching point

Compatibility for the deflections, slopes, and moments at the attaching point requires that

$$\bar{Y}^L_v(\xi_v) = \bar{Y}^R_v(\xi_v) \tag{13a}$$

$$\bar{Y}'^L_v(\xi_v) = \bar{Y}'^R_v(\xi_v) \tag{13b}$$

$$\bar{Y}''^L_v(\xi_v) + \frac{k^*_{Rv}}{(\alpha-1)\xi^4_v}\bar{Y}'^L_v(\xi_v) = \bar{Y}''^R_v(\xi_v) \tag{13c}$$

From the force equilibrium at the attaching point, one has

$$4(\alpha-1)^3\xi^3\bar{Y}''^L_v(\xi_v) + (\alpha-1)^3\xi^4\bar{Y}'''^L_v(\xi_v) - \left\{k^*_{Tv} - m^*_{cv}\left[\frac{1}{3}(\alpha-1)^2 + \alpha\right](\Omega L)^4\right\}\bar{Y}^L_v(\xi_v)$$
$$= 4(\alpha-1)^3\xi^3\bar{Y}''^R_v(\xi_v) + (\alpha-1)^3\xi^4\bar{Y}'''^R_v(\xi_v) \tag{14}$$

where

$$k^*_{Rv} = \frac{k_{Rv}L}{EI_0} \tag{15}$$

$$k^*_{Tv} = \frac{k_{Tv}L^3}{EI_0} \tag{16}$$

$$m^*_{cv} = \frac{m_{cv}}{m_b} = \frac{m_{cv}}{\rho A_0 L\left[\frac{1}{3}(\alpha-1)^2 + (\alpha-1) + 1\right]} \tag{17}$$

where m_{cv} (or k_{Tv} or k_{Rv}) represents the v-th rigidly-attached concentrated mass (or translational spring or rotational spring) and $m_b = \rho A_0 L[1/3(\alpha-1)^2 + (\alpha-1) + 1]$ is the total mass of the beam.

The substitution of Eqs. (8)~(12) into Eqs. (13) and (14) leads to

$$C_{v1}J_2(\beta\sqrt{\xi_v}) + C_{v2}Y_2(\beta\sqrt{\xi_v}) + C_{v3}I_2(\beta\sqrt{\xi_v}) + C_{v4}K_2(\beta\sqrt{\xi_v})$$
$$- C_{v+1,1}J_2(\beta\sqrt{\xi_v}) - C_{v+1,2}Y_2(\beta\sqrt{\xi_v}) - C_{v+1,3}I_2(\beta\sqrt{\xi_v}) - C_{v+1,4}K_2(\beta\sqrt{\xi_v}) = 0 \tag{18a}$$

$$C_{v1}J_3(\beta\sqrt{\xi_v}) + C_{v2}Y_3(\beta\sqrt{\xi_v}) - C_{v3}I_3(\beta\sqrt{\xi_v}) + C_{v4}K_3(\beta\sqrt{\xi_v})$$
$$- C_{v+1,1}J_3(\beta\sqrt{\xi_v}) - C_{v+1,2}Y_3(\beta\sqrt{\xi_v}) + C_{v+1,3}I_3(\beta\sqrt{\xi_v}) - C_{v+1,4}K_3(\beta\sqrt{\xi_v}) = 0 \tag{18b}$$

$$\left[\frac{\beta}{2}\right]^2\xi_v^{-2}[C_{v1}J_4(\beta\sqrt{\xi_v}) + C_{v2}Y_4(\beta\sqrt{\xi_v}) + C_{v3}I_4(\beta\sqrt{\xi_v}) + C_{v4}K_4(\beta\sqrt{\xi_v})]$$
$$-\frac{k^*_{Rv}}{(\alpha-1)}\left(\frac{\beta}{2}\right)\xi_v^{-11/2}[C_{v1}J_3(\beta\sqrt{\xi_v}) + C_{v2}Y_3(\beta\sqrt{\xi_v}) - C_{v3}I_3(\beta\sqrt{\xi_v}) + C_{v4}K_3(\beta\sqrt{\xi_v})]$$
$$-\left[\frac{\beta}{2}\right]^2\xi_v^{-2}[C_{v+1,1}J_4(\beta\sqrt{\xi_v}) + C_{v+1,2}Y_4(\beta\sqrt{\xi_v}) + C_{v+1,3}I_4(\beta\sqrt{\xi_v}) + C_{v+1,4}K_4(\beta\sqrt{\xi_v})] = 0 \tag{18c}$$

$$\begin{aligned}
&8\beta^2[C_{\nu 1}J_4(\beta\sqrt{\xi_\nu}) + C_{\nu 2}Y_4(\beta\sqrt{\xi_\nu}) + C_{\nu 3}I_4(\beta\sqrt{\xi_\nu}) + C_{\nu 4}K_4(\beta\sqrt{\xi_\nu})]\\
&-\beta^3\xi_\nu^{1/2}[C_{\nu 1}J_5(\beta\sqrt{\xi_\nu}) + C_{\nu 2}Y_5(\beta\sqrt{\xi_\nu}) - C_{\nu 3}I_5(\beta\sqrt{\xi_\nu}) + C_{\nu 4}K_5(\beta\sqrt{\xi_\nu})]\\
&-8\theta_\nu\xi_\nu^{-2}[C_{\nu 1}J_2(\beta\sqrt{\xi_\nu}) + C_{\nu 2}Y_2(\beta\sqrt{\xi_\nu}) + C_{\nu 3}I_2(\beta\sqrt{\xi_\nu}) + C_{\nu 4}K_2(\beta\sqrt{\xi_\nu})]\\
&-8\beta^2[C_{\nu+1,1}J_4(\beta\sqrt{\xi_\nu}) + C_{\nu+1,2}Y_4(\beta\sqrt{\xi_\nu}) + C_{\nu+1,3}I_4(\beta\sqrt{\xi_\nu}) + C_{\nu+1,4}K_4(\beta\sqrt{\xi_\nu})]\\
&+\beta^3\xi_\nu^{1/2}[C_{\nu+1,1}J_5(\beta\sqrt{\xi_\nu}) + C_{\nu+1,2}Y_5(\beta\sqrt{\xi_\nu}) - C_{\nu+1,3}I_5(\beta\sqrt{\xi_\nu}) + C_{\nu+1,4}K_5(\beta\sqrt{\xi_\nu})] = 0
\end{aligned} \tag{18d}$$

where

$$\theta_\nu = \frac{k_{T\nu}^*}{(\alpha-1)^3} - \frac{m_{c\nu}^*\left[\frac{1}{3}(\alpha-1)^2+\alpha\right](\Omega L)^4}{(\alpha-1)^3} \tag{18e}$$

It is noted that, in Eqs. (13) and (14), the "left side" of the ν-th attaching point located at $x = x_\nu$ belongs to the segment (ν) and the "right side" belongs to the segment ($\nu+1$), thus the associated coefficients are represented by $C_{\nu i}$ and $C_{\nu+1,\,i}$ (i = 1~4), respectively, as may be seen from Eqs. (18a)~(18d).

To write Eqs. (18a)~(18d) in matrix form gives

$$[B_\nu]\{C_\nu\} = \{0\} \tag{19}$$

where

$$\begin{aligned}
\{C_\nu\} &= \{C_{\nu 1}\ \ C_{\nu 2}\ \ C_{\nu 3}\ \ C_{\nu 4}\ \ C_{\nu+1,1}\ \ C_{\nu+1,2}\ \ C_{\nu+1,3}\ \ C_{\nu+1,4}\}\\
&= \{\bar{C}_{4\nu-3}\ \ \bar{C}_{4\nu-2}\ \ \bar{C}_{4\nu-1}\ \ \bar{C}_{4\nu}\ \ \bar{C}_{4\nu+1}\ \ \bar{C}_{4\nu+2}\ \ \bar{C}_{4\nu+3}\ \ \bar{C}_{4\nu+4}\}
\end{aligned} \tag{20a}$$

$$\bar{C}_{4\nu-3} = C_{\nu 1},\quad \bar{C}_{4\nu-2} = C_{\nu 2},\ \ldots,\quad \bar{C}_{4\nu+4} = C_{\nu+1,4} \tag{20b}$$

and

$$[B_\nu] = \begin{array}{cc}
\begin{matrix} 4\nu-3 & 4\nu-2 & 4\nu-1 & 4\nu & 4\nu+1 & 4\nu+2 & 4\nu+3 & 4\nu+4 \end{matrix} & \\
\begin{bmatrix}
J_2(\delta_\nu) & Y_2(\delta_\nu) & I_2(\delta_\nu) & K_2(\delta_\nu) & -J_2(\delta_\nu) & -Y_2(\delta_\nu) & -I_2(\delta_\nu) & -K_2(\delta_\nu)\\
J_3(\delta_\nu) & Y_3(\delta_\nu) & -I_3(\delta_\nu) & K_3(\delta_\nu) & -J_3(\delta_\nu) & -Y_3(\delta_\nu) & I_3(\delta_\nu) & -K_3(\delta_\nu)\\
\nabla_{1\nu} & \nabla_{2\nu} & \nabla_{3\nu} & \nabla_{4\nu} & -\nabla_{5\nu} & -\nabla_{6\nu} & -\nabla_{7\nu} & -\nabla_{8\nu}\\
\Delta_{1\nu} & \Delta_{2\nu} & \Delta_{3\nu} & \Delta_{4\nu} & -\Delta_{5\nu} & -\Delta_{6\nu} & -\Delta_{7\nu} & -\Delta_{8\nu}
\end{bmatrix} & \begin{matrix} 4\nu-1 \\ 4\nu \\ 4\nu+1 \\ 4\nu+2 \end{matrix}
\end{array} \tag{20c}$$

where

$$\nabla_{1\nu} = \beta^2 J_4(\delta_\nu) - \frac{2k_{R\nu}^*}{(\alpha-1)}\beta\xi_\nu^{-7/2}J_3(\delta_\nu),\qquad \nabla_{2\nu} = \beta^2 J_4(\delta_\nu) - \frac{2k_{R\nu}^*}{(\alpha-1)}\beta\xi_\nu^{-7/2}Y_3(\delta_\nu),$$

$$\nabla_{3\nu} = \beta^2 I_4(\delta_\nu) + \frac{2k_{R\nu}^*}{(\alpha-1)}\beta\xi_\nu^{-7/2}I_3(\delta_\nu),\qquad \nabla_{4\nu} = \beta^2 K_4(\delta_\nu) - \frac{2k_{R\nu}^*}{(\alpha-1)}\beta\xi_\nu^{-7/2}K_3(\delta_\nu),$$

$$\nabla_{5\nu} = \beta^2 J_4(\delta_\nu),\qquad \nabla_{6\nu} = \beta^2 Y_4(\delta_\nu),\qquad \nabla_{7\nu} = \beta^2 I_4(\delta_\nu),\qquad \nabla_{8\nu} = \beta^2 K_4(\delta_\nu),$$

$$\delta_\nu = \beta\sqrt{\xi_\nu},\qquad \Delta_{1\nu} = 8\beta^2 J_4(\beta\sqrt{\xi_\nu}) - \beta^3\xi_\nu^{1/2}J_5(\beta\sqrt{\xi_\nu}) - 8\theta_\nu\xi_\nu^{-2}J_2(\beta\sqrt{\xi_\nu}),$$

$$\Delta_{2\nu} = 8\beta^2 Y_4(\beta\sqrt{\xi_\nu}) - \beta^3\xi_\nu^{1/2} Y_5(\beta\sqrt{\xi_\nu}) - 8\theta_\nu\xi_\nu^{-2} Y_2(\beta\sqrt{\xi_\nu}),$$

$$\Delta_{3\nu} = 8\beta^2 I_4(\beta\sqrt{\xi_\nu}) + \beta^3\xi_\nu^{1/2} I_5(\beta\sqrt{\xi_\nu}) - 8\theta_\nu\xi_\nu^{-2} I_2(\beta\sqrt{\xi_\nu}),$$

$$\Delta_{4\nu} = 8\beta^2 K_4(\beta\sqrt{\xi_\nu}) - \beta^3\xi_\nu^{1/2} K_5(\beta\sqrt{\xi_\nu}) - 8\theta_\nu\xi_\nu^{-2} K_2(\beta\sqrt{\xi_\nu}),$$

$$\Delta_{5\nu} = 8\beta^2 J_4(\beta\sqrt{\xi_\nu}) - \beta^3\xi_\nu^{1/2} J_5(\beta\sqrt{\xi_\nu}), \qquad \Delta_{6\nu} = 8\beta^2 Y_4(\beta\sqrt{\xi_\nu}) - \beta^3\xi_\nu^{1/2} Y_5(\beta\sqrt{\xi_\nu}),$$

$$\Delta_{7\nu} = 8\beta^2 I_4(\beta\sqrt{\xi_\nu}) + \beta^3\xi_\nu^{1/2} I_5(\beta\sqrt{\xi_\nu}), \qquad \Delta_{8\nu} = 8\beta^2 K_4(\beta\sqrt{\xi_\nu}) - \beta^3\xi_\nu^{1/2} K_5(\beta\sqrt{\xi_\nu}) \quad (20d)$$

4. Coefficient matrix [B_L] for the left end of the beam

For a cantilever beam with left end clamped, the boundary conditions are

$$\bar{Y}(1) = 0, \qquad \bar{Y}'(1) = 0 \quad (21a),(21b)$$

From Fig. 1 one sees that the left end of the beam, L, coincides with the left end of the first beam segment ($\nu = 1$), hence from Eqs. (8), (9), (21a) and (21b) one obtains

$$J_2(\beta)C_{11} + Y_2(\beta)C_{12} + I_2(\beta)C_{13} + K_2(\beta)C_{14} = 0 \quad (22a)$$

$$J_3(\beta)C_{11} + Y_3(\beta)C_{12} - I_3(\beta)C_{13} + K_3(\beta)C_{14} = 0 \quad (22b)$$

To write the last two expressions in matrix form gives

$$[B_L]\{C_L\} = \{0\} \quad (23)$$

where

$$[B_L] = \begin{array}{cc} \begin{array}{cccc} 1 & 2 & 3 & 4 \end{array} & \\ \begin{bmatrix} J_2(\beta) & Y_2(\beta) & I_2(\beta) & K_2(\beta) \\ J_3(\beta) & Y_3(\beta) & -I_3(\beta) & K_3(\beta) \end{bmatrix} & \begin{array}{c} 1 \\ 2 \end{array} \end{array} \quad (24)$$

$$\{C_L\} = \{C_{11}\ C_{12}\ C_{13}\ C_{14}\} = \{\bar{C}_1\ \bar{C}_2\ \bar{C}_3\ \bar{C}_4\} \quad (25)$$

where the [ ] and { } represent the rectangular matrix and the column vector, respectively, and

$$\bar{C}_1 = C_{11}, \qquad \bar{C}_2 = C_{12}, \qquad \bar{C}_3 = C_{13}, \qquad \bar{C}_4 = C_{14} \quad (26)$$

In Eq. (24) and the subsequent equations, the digits shown on the top side and right side of the matrix represent the identification numbers of degrees of freedom (dof) for the associated constants $\bar{C}_i$ (i = 1, 2, ...).

5. Coefficient matrix [B_R] for the right end of the beam

For a cantilever beam with right end free, the boundary conditions are

$$\bar{Y}''(\alpha) = 0, \qquad 4\alpha^{-1}\bar{Y}''(\alpha) + \bar{Y}'''(\alpha) = 0 \quad (27a),(27b)$$

Since the right end of the beam, R, coincides with the right end of the $(n+1)$-th segment $(v = n+1)$, as one may see from Fig. 1, hence from Eqs. (11), (12), (27a) and (27b) one obtains

$$J_4(\beta\sqrt{\alpha})C_{n+1,1} + Y_4(\beta\sqrt{\alpha})C_{n+1,2} + I_4(\beta\sqrt{\alpha})C_{n+1,3} + K_4(\beta\sqrt{\alpha})C_{n+1,4} = 0 \tag{28a}$$

$$\begin{aligned}&[8J_4(\beta\sqrt{\alpha}) - \beta\alpha^{1/2}J_5(\beta\sqrt{\alpha})]C_{n+1,1} + [8Y_4(\beta\sqrt{\alpha}) - \beta\alpha^{1/2}Y_5(\beta\sqrt{\alpha})]C_{n+1,2}\\ &+ [8I_4(\beta\sqrt{\alpha}) + \beta\alpha^{1/2}I_5(\beta\sqrt{\alpha})]C_{n+1,3} + [8K_4(\beta\sqrt{\alpha}) - \beta\alpha^{1/2}K_5(\beta\sqrt{\alpha})]C_{n+1,4} = 0\end{aligned} \tag{28b}$$

To write Eqs. (28a) and (28b) in matrix form gives

$$[B_R]\{C_R\} = \{0\} \tag{29}$$

where

$$[B_R] = \begin{array}{cc} \begin{array}{cccc} 4n+1 & 4n+2 & 4n+3 & 4n+4 \end{array} & \\ \begin{bmatrix} J_4(\beta\sqrt{\alpha}) & Y_4(\beta\sqrt{\alpha}) & I_4(\beta\sqrt{\alpha}) & K_4(\beta\sqrt{\alpha}) \\ \varepsilon_1 & \varepsilon_2 & \varepsilon_3 & \varepsilon_4 \end{bmatrix} & \begin{array}{c} p-1 \\ p \end{array} \end{array} \tag{30a}$$

$$\begin{aligned}\varepsilon_1 &= [8J_4(\beta\sqrt{\alpha}) - \beta\alpha^{1/2}J_5(\beta\sqrt{\alpha})], \qquad \varepsilon_2 = [8Y_4(\beta\sqrt{\alpha}) - \beta\alpha^{1/2}Y_5(\beta\sqrt{\alpha})],\\ \varepsilon_3 &= [8I_4(\beta\sqrt{\alpha}) + \beta\alpha^{1/2}I_5(\beta\sqrt{\alpha})], \qquad \varepsilon_4 = [8K_4(\beta\sqrt{\alpha}) - \beta\alpha^{1/2}K_5(\beta\sqrt{\alpha})]\end{aligned} \tag{30b}$$

$$\begin{aligned}\{C_R\} &= \{C_{n+1,1} \;\; C_{n+1,2} \;\; C_{n+1,3} \;\; C_{n+1,4}\}\\ &= \{\bar{C}_{4n+1} \;\; \bar{C}_{4n+2} \;\; \bar{C}_{4n+3} \;\; \bar{C}_{4n+4}\}\end{aligned} \tag{31}$$

$$\bar{C}_{4n+1} = C_{n+1,1}, \quad \bar{C}_{4n+2} = C_{n+1,2}, \quad \bar{C}_{4n+3} = C_{n+1,3}, \quad \bar{C}_{4n+4} = C_{n+1,4} \tag{32}$$

$$p = 4n + 4 \tag{33}$$

In the last equations, p represents the total number of equations. From the above derivations one sees that from each attaching point for a concentrated element one may obtain four equations (including three compatibility equations and one force-equilibrium equation) and from each boundary (L or R) one may obtain two equations. Hence, for a beam carrying n concentrated elements, the total number of equations that one may obtain for the integration constants $C_{vi}(v = 1\sim n,\ i = 1\sim 4)$ is equal to $4n+4$, i.e., $p = 4n+4$ as shown by Eq. (33). Of course, the total number of unknowns (C_{vi}) is also equal to $4n+4$. From Eq. (8) one sees that the solution $\bar{Y}_v(\xi)$ for each beam segment contain four unknown integration constants $C_{vi}(i = 1\sim 4)$, hence if a beam carries n concentrated elements, then the total number of the beam segment is $n+1$ and thus the total number of unknown (C_{vi}) is equal to $4(n+1) = 4n+4 = p$.

6. Overall coefficient matrix $[\bar{B}]$ of the entire beam and the frequency equation

If all the unknowns $C_{vi}(v = 1\sim n,\ i = 1\sim 4)$ are replaced by a column vector $\{C\}$ with coefficients $C_k(k = 1, 2, ..., p)$ defined by Eqs. (26), (20b) and (32), then the matrices $[B_L]$, $[B_v]$ and $[B_R]$ are similar to the element property matrices (for the finite element method) with corresponding identification numbers for the degrees of freedom (dof) shown on the top side and right side of the matrices defined by Eqs. (20c), (24) and (30a). Basing on the assembly technique for the direct stiffness matrix method, it is easy to arrive at the following coefficient equation for the entire vibrating system

$$[B]\{C\} = \{0\} \tag{34}$$

Nontrivial solution of the problem requires that

$$|B| = 0 \tag{35}$$

which is the frequency equation, and the half-interval technique [Faires and Burden 1993] may be used to solve the eigenvalues $\bar{\omega}_j\,(j = 1, 2, ...)$. To substitute each value of $\bar{\omega}_j$ into Eq. (34) one may determine the values of unknowns $C_k(k = 1, 2, ..., p)$. Among which, from Eq. (26) one sees that $\bar{C}_{4v-3} = C_{v1}$, $\bar{C}_{4v-2} = C_{v2}$, $\bar{C}_{4v-1} = C_{v3}$, $\bar{C}_{4v} = C_{v4}$, $v = 1\sim n$, hence the substitution of $C_{vi}(i = 1\sim4)$ into Eq. (8) will define the corresponding mode shape $\bar{Y}^{(j)}(\xi)$. For a cantilever beam carrying one ($n = 1$) and two ($n = 2$) concentrated elements, the corresponding overall coefficient matrices $[B]_{(1)}$ and $[B]_{(2)}$ were shown in Appendix 1 [see Eqs. (A1) and (A2)]. From the lengthy expressions one sees that the conventional explicit formulations are not suitable for a beam carrying more than two ($n > 2$) concentrated elements. However this is not true for the numerical assembly method (NAM) adopted in this paper.

7. Coefficient matrices [B_L] and [B_R] for various boundary conditions

From the previous sections one finds that the form of the coefficient matrix [B_v] for each attaching point of the concentrated element has nothing to do with the boundary conditions of the beam, hence for a "constrained" beam with various supporting conditions the only thing one should do is to modify the values of the two boundary matrices [B_L] and [B_R] defined by Eqs. (24) and (30a), respectively, according to the actual boundary conditions. And then the same numerical assembly procedures introduced in the last section may be followed. This is one of the predominant advantages of the NAM. The boundary matrices [B_L] and [B_R] for various boundary conditions were placed in Appendix 2 at the end of this paper.

8. Numerical results and discussions

The dimensions and physical properties of the doubly-tapered beam studied in this paper are: $L = 40$ in, $E = 3.0 \times 10^7$ psi, $A_0 = 1.5$ in^2, $I_0 = 0.28125$ in^4, $\rho = 0.283$ lbm, $\alpha = 2.0$, $m_b = \rho A_0 L$ $[1/3(\alpha - 1)^2 + (\alpha - 1) + 1] = 29.715$ lbm, $k_b = EI_0/L^3 = 312.5$ lbf/in.

For convenience, three non-dimensional parameters for each concentrated element were introduced : $m^*_{ci} = m_{ci}/m_b$, $k^*_{Ti} = k_{Ti}/k_b$ and $k^*_{Ri} = k_{Ri}/(EI_0/L)$, $i = 1, 2, \ldots, n$. In addition, the two-letter acronyms, FC, CF, SC, CS, CC and SS, were used to denote the free-clamped (FC), clamped-free (CF), simply supported-clamped (SC), clamped-simply supported (CS), clamped-clamped (CC), and simply supported-simply supported (SS) boundary conditions of the beam, respectively.

8.1 Comparing with the existing results

In order to compare the results of NAM with the corresponding ones of De Rosa and Auciello

(1996), the “unconstrained” SS and FC tapered beams (without carrying any concentrated elements) were studied first. The lowest four non-dimensional frequency coefficients, Ω_j ($j = 1 \sim 4$), with the taper ratios $\alpha = 2.0$ and $\alpha = 1.4$, respectively, were shown in Table 1. It is evident that the results of the introduced method (NAM) and those of De Rosa and Auciello (1996) are in good agreement.

For the case of the tapered cantilever beam carrying “a single” translational spring at its free end and with a taper ratio $\alpha = 2.0$, Table 2 shows the lowest four non-dimensional frequency coefficients, $\overline{\Omega}_j$ ($j = 1 \sim 4$), obtained from the NAM and those from De Rosa and Auciello (1996). It is also found that the values of $\overline{\Omega}_j$ ($j = 1 \sim 4$) obtained from the NAM are very close to those of De Rosa and Auciello (1996). According to the above comparison results, it is believed that the adopted method (NAM) in this paper is robust and accurate.

Table 1 The lowest four non-dimensional frequency coefficients Ω_j ($j = 1 \sim 4$) for the “unconstrained” non-uniform beam (without carrying any concentrated elements) with the support conditions: SS and FC

Boundary conditions	Taper ratios α	Methods	Non-dimensional frequency coefficients			
			Ω_1	Ω_2	Ω_3	Ω_4
SS	2.0	NAM	3.7300	7.6302	11.4217	15.2083
		De Rosa and Auciello (1996)	3.7300	7.6302	11.4217	15.2083
FC	1.4	NAM	2.3766	5.3739	8.7264	12.1135
		De Rosa and Auciello (1996)	2.3766	5.3739	8.7264	12.1135

*NAM = numerical assembly method

Table 2 The lowest four non-dimensional frequency coefficients $\overline{\Omega}_j$($j = 1 \sim 4$) for the FC tapered beam carrying “a single” translational spring at its free end and with a taper ratio $\alpha = 2.0$

$k_{T1}^* = \frac{k_{T1}}{k_b}$	Methods	Non-dimensional frequency coefficients			
		$\overline{\Omega}_1$	$\overline{\Omega}_2$	$\overline{\Omega}_3$	$\overline{\Omega}_4$
10.0	NAM	2.85540	5.44142	8.74258	12.11962
	De Rosa and Auciello (1996)	2.85540	5.44140	8.74260	12.11960
1.0	NAM	2.44201	5.38055	8.72799	12.11413
	De Rosa and Auciello (1996)	2.44200	5.38050	8.72800	12.11410
0.1	NAM	2.38344	5.37454	8.72654	12.11358
	De Rosa and Auciello (1996)	2.38340	5.37450	8.72650	12.11360

*NAM = numerical assembly method

8.2 Free vibration analysis of the “unconstrained” tapered beam

Since the information regarding the natural frequencies and mode shapes of a doubly-tapered beam carrying multiple concentrated elements has not been found yet, the numerical results of this paper are compared with those obtained from the conventional finite element method (FEM) to confirm their reliability. To this end, the above-mentioned tapered beam was replaced by a stepped beam as shown in Fig. 2. Table 3(a) shows the influence of the total number of beam elements for FC unconstrained doubly-tapered beam (with taper ratio $\alpha = 2.0$), N_e, on the lowest five natural frequencies obtained from FEM. From the table one sees that the FEM results are very close to the corresponding "exact" solutions obtained from application of Bessel's functions when $N_e \approx 60$. For this reason, the FEM results of this paper were obtained based on N_e = 60. The cross-sectional area A_i and the moment of inertia I_i of the i-th "uniform beam segment" for the stepped beam shown in Fig. 2 are equal to the average values of the corresponding ones for the i-th "tapered beam segment", respectively, and the mass per unit length of the i-th uniform beam segment is evaluated by ρA_i. The length of each uniform beam segment is $l = L/60$ = 2/3 in for the case of N_e = 60.

In Table 3(b) and the subsequent Tables, the same doubly-tapered beam (taper ratio $\alpha = 2.0$) with six boundary conditions (i.e., FC, CF, SC, CS, CC and SS) were studied. From Table 3(b) one sees that the NAM results and FEM results are very close to each other. In Fig. 3 one sees that the node number N_{mj} for the j-th mode shape of the six types of boundary conditions of the beam are given by $N_{mj} = j - 1$. It is noteworthy in Fig. 3 that the modal displacements near the left ends of the SC, CS, CC or SS tapered beam are larger than those near the right end of the beam. This is reasonable, because the stiffness of the left end is much smaller than that of the right end of each tapered beam as one may see from Fig. 1 and Fig. 2.

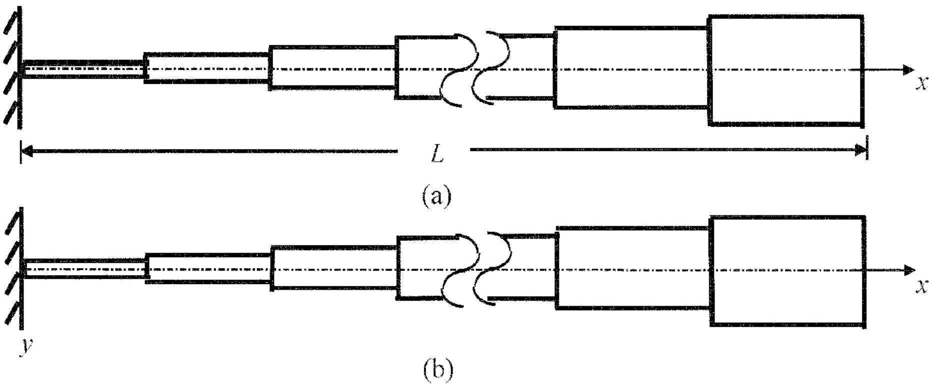

Fig. 2 The finite element model for the doubly-tapered beam: (a) Top view and (b) Front view

Table 3(a) Influence of number of beam elements (N_e) on the lowest five natural frequencies of the CF unconstrained doubly-tapered beam using FEM

Number of elements, N_e	Natural frequencies (rad/sec)				
	ω_1	ω_2	ω_3	ω_4	ω_5
40	7.23856	73.51321	236.92092	477.81289	798.75291
50	7.23694	73.50012	236.88221	477.73541	798.62131
60	7.23607	73.49300	236.86116	477.69338	798.55044
70	7.23554	73.48871	236.84846	477.66806	798.50792
# Exact sol.	7.23408	73.47681	236.81331	477.59822	798.39106

#The exact solutions were obtained from NAM (without concentrated elements).

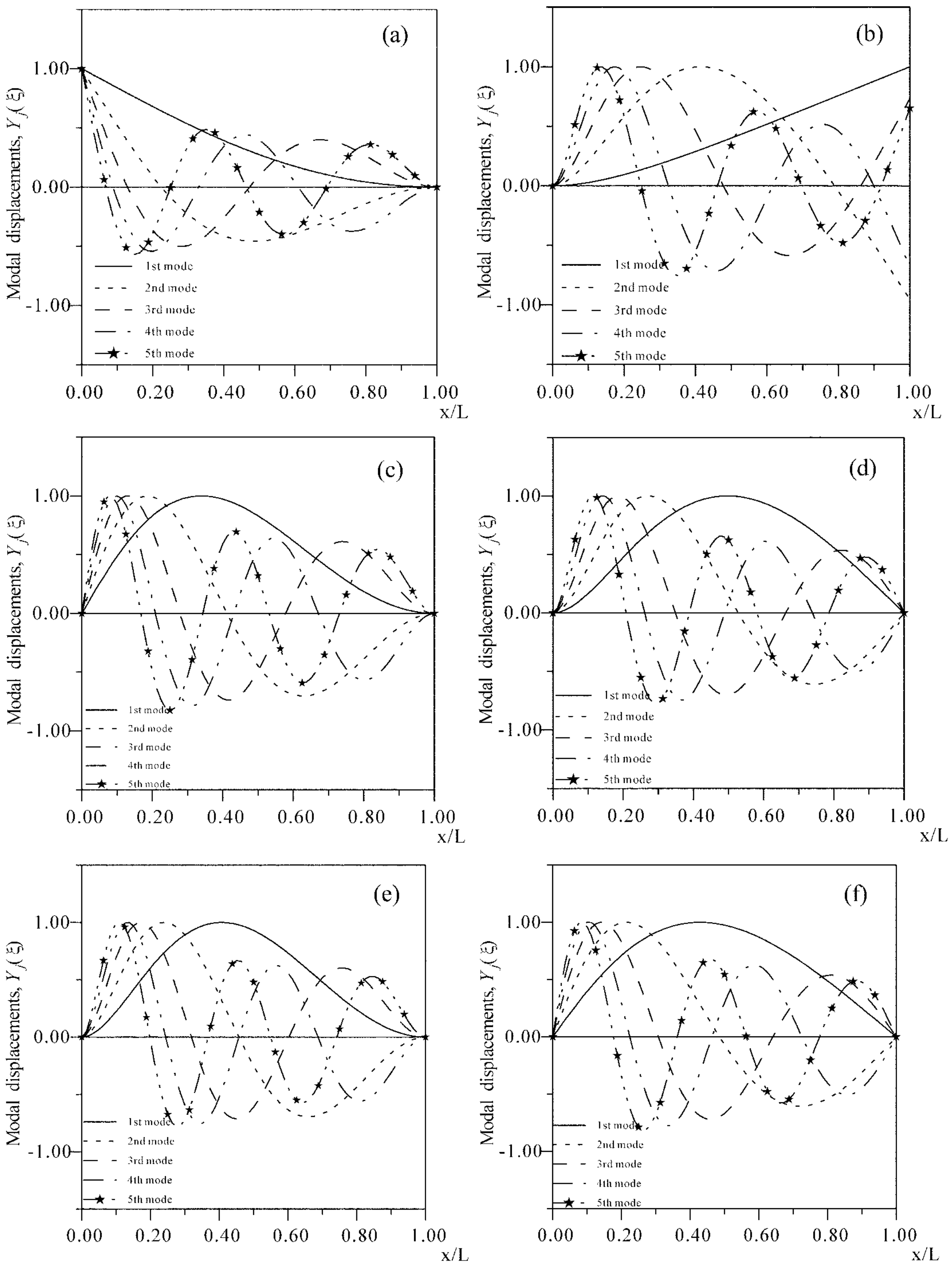

Fig. 3 The lowest five mode shapes $Y_j(\xi)$ (j = 1~5) for the "unconstrained" doubly-tapered beam (without carrying any concentrated elements) with the support conditions: (a) FC, (b) CF, (c) SC, (d) CS, (e) CC and (f) SS

8.3 Free vibration analysis of the "constrained" tapered beam

Case 1: carrying five point masses

For the tapered beam carrying five point masses with locations and magnitudes shown in Table 4,

Table 3(b) The lowest five natural frequencies $\omega_j (j = 1\sim5)$ for the "unconstrained" doubly-tapered beam (without carrying any concentrated elements)

Boundary conditions	Methods	Natural frequencies (rad/sec)				
		ω_1	ω_2	ω_3	ω_4	ω_5
FC	NAM	25.77532	108.93610	270.72329	511.65966	832.52916
	FEM	25.77957	108.96115	270.79725	511.80228	832.79109
CF	NAM	7.23408	73.47681	236.81331	477.59822	798.39106
	FEM	7.23607	73.49300	236.86116	477.69338	798.55044
SC	NAM	71.61388	212.87668	433.85401	734.70179	1115.57882
	FEM	71.62427	212.91674	433.93632	734.84742	1115.82269
CS	NAM	53.77585	196.23185	417.05549	717.82045	1098.63870
	FEM	53.78521	196.26335	417.12164	717.93454	1098.81537
CC	NAM	91.83540	251.75856	492.37771	813.02661	1213.79486
	FEM	91.84257	251.77828	492.41639	813.09170	1213.89496
SS	NAM	38.76810	162.22786	363.50517	644.48275	1005.41779
	FEM	38.76997	162.23740	363.53147	644.54148	1005.51533

*NAM = numerical assembly method; FEM = finite element method

Table 4 The locations and magnitudes of the four kinds of concentrated attachments

Concentrated attachments	Locations of point masses and/or translational springs and/or rotational springs $\xi_j = x_j/L$					Magnitudes of translational spring constants $k^*_{Ti} = k_{Ti}/k_b$					Magnitudes of rotational spring constants $k^*_{Ri} = k_{Ri}/(EI_0/L)$					Magnitudes of point masses $m^*_{ci} = m_{ci}/m_b$					Remarks
	ξ_1	ξ_2	ξ_3	ξ_4	ξ_5	k^*_{T1}	k^*_{T2}	k^*_{T3}	k^*_{T4}	k^*_{T5}	k^*_{R1}	k^*_{R2}	k^*_{R3}	k^*_{R4}	k^*_{R5}	m^*_{c1}	m^*_{c2}	m^*_{c3}	m^*_{c4}	m^*_{c5}	
Point masses m^*_{ci}	0.1	0.3	0.5	0.7	0.9											0.2	0.2	0.2	0.2	0.2	Case1
Translational springs k^*_{Ti}	0.1	0.3	0.5	0.7	0.9	1.0	1.0	1.0	1.0	1.0											Case2
Rotational springs k^*_{Ri}	0.1	0.3	0.5	0.7	0.9						1.0	1.0	1.0	1.0	1.0						Case3
Point masses m^*_{ci}, translational springs k^*_{Ti} and rotational springs k^*_{Ri}	0.1	0.3	0.5	0.7	0.9	1.0	1.0	1.0	1.0	1.0	1.0	1.0	1.0	1.0	1.0	0.2	0.2	0.2	0.2	0.2	Case4 (Combination of Case1, Case2 and Case3)

the calculated lowest five natural frequencies $\bar{\omega}_j\,(j=1\sim5)$ were shown in Table 5 and the corresponding mode shapes $\bar{Y}_j\,(j=1\sim5)$ for the six types of boundary conditions were shown in Figs. 4(a)~4(f), respectively. It can be seen that the lowest five natural frequencies of the "constrained" beam, $\bar{\omega}_j\,(j=1\sim5)$, shown in Table 5 are smaller than the corresponding ones of the "unconstrained" beam, $\omega_j(j=1\sim5)$, shown in Table 2. The difference between $\bar{\omega}_j$ and ω_j, $\Delta\omega_j = \omega_j - \bar{\omega}_j$, increases with increasing the mode number j. But the lowest five mode shapes of the "constrained" beam shown in Fig. 4 look like those of the "unconstrained" beam shown in Fig. 3. The five "identical" point masses "uniformly" distributed along the beam length should be the main reason arriving at the last result.

The percentage differences between $\bar{\omega}_{jNAM}$ and $\bar{\omega}_{jFEM}$ shown in the parentheses ( ) of Table 5 were calculated with the formula: $\varepsilon_j^* = (\bar{\omega}_{jFEM} - \bar{\omega}_{jNAM}) \times 100\% / \bar{\omega}_{jFEM}$, where $\bar{\omega}_{jNAM}$ and $\bar{\omega}_{jFEM}$ denote the j-th natural frequencies of the "constrained" beam obtained from the NAM and the FEM, respectively. In Table 5 one finds that the maximum value of ε_j is $\varepsilon_5^* = 0.0667\%$ (for the FC boundary condition), hence the accuracy of the NAM is good.

Case 2: carrying five translational springs

For the same tapered beam carrying five translational springs with locations and magnitudes shown in Table 4, the lowest five natural frequencies $\bar{\omega}_j\,(j=1\sim5)$ of the constrained beam were shown in Table 6. Comparing with the results of Table 6 and Table 2, one sees that the lowest five natural frequencies of the "unconstrained" beam, $\omega_j\,(j=1\sim5)$, shown in Table 2 are smaller than the corresponding ones of the "constrained" beam, $\bar{\omega}_j\,(j=1\sim5)$, shown in Table 6. Furthermore, the maximum value of the percentage difference between $\bar{\omega}_{jNAM}$ and $\bar{\omega}_{jFEM}$ $(j=1\sim5)$ is $\varepsilon_4^* = 0.0324\%$ (for the CF beam), hence the accuracy of the NAM is excellent for the present case. Since the corresponding mode shapes for the "constrained" beams are almost coincident with the ones for the "unconstrained" beams, the former were not shown in this paper.

Case 3: carrying five rotational springs

For the same tapered beam carrying five rotational springs with locations and magnitudes given in Table 4, the lowest five natural frequencies $\bar{\omega}_j\,(j=1\sim5)$ were shown in Table 7. From Table 7 and Table 2 it is seen also that the lowest five natural frequencies of the "unconstrained" beam are smaller than the corresponding ones of the "constrained" beam. The maximum value of the percentage difference is found to be $\varepsilon_5^* = 0.0469\%$ (for the FC beam). The corresponding mode shapes for the "constrained" beam are also almost identical with the ones for the "unconstrained" beam and not shown here.

Case 4: carrying five point masses, five translational springs and five rotational springs

Finally, the tapered beam carrying five point masses, five translational springs and five rotational springs, a combination of Case1, Case2 and Case3, is studied. The computed lowest five natural frequencies $\bar{\omega}_j\,(j=1\sim5)$ were shown in Table 8 and it is interesting that the values of $\bar{\omega}_j$ for the present Case 4 are very close to those for Case 1, where the tapered beam carries five point masses alone. This is the reason that the corresponding mode shapes of the present case (see Fig. 5) are almost the same as the lowest five mode shapes of the tapered beam of the Case 1 (see Fig. 4). It is noted that only the lowest five mode shapes of the tapered beam with FC, CF and SC were shown in Fig. 5.

Table 5 The lowest five natural frequencies for the doubly-tapered beam carrying five point masses with locations and magnitudes shown in Table 4 (Case 1)

Boundary conditions	Methods	Natural frequencies (rad/sec)				
		$\bar{\omega}_1$	$\bar{\omega}_2$	$\bar{\omega}_3$	$\bar{\omega}_4$	$\bar{\omega}_5$
FC	NAM	15.89633 (0.0059%)	73.69710 (0.0137%)	192.03138 (0.0173%)	384.84166 (0.0363%)	682.50090 (0.0667%)
	FEM	15.89728	73.70723	192.99816	384.98167	682.95681
CF	NAM	5.52700 (0.0204%)	52.35275 (0.0223%)	165.56475 (0.0279%)	336.91485 (0.0341%)	480.72236 (0.0345%)
	FEM	5.52813	52.36443	165.61112	337.03006	480.88865
SC	NAM	48.02431 (0.0248%)	142.94833 (0.0259%)	280.18354 (0.0261%)	434.93220 (0.0263%)	886.24478 (0.0607%)
	FEM	48.03623	142.98542	280.25657	435.04620	886.78312
CS	NAM	37.94101 (0.0191%)	134.90981 (0.0215%)	288.55991 (0.0245%)	449.57620 (0.0440%)	664.70462 (0.0441%)
	FEM	37.94829	134.93887	288.63082	449.77431	664.99837
CC	NAM	62.95041 (0.0107%)	172.69856 (0.0114%)	339.87602 (0.0242%)	480.22513 (0.0292%)	891.00593 (0.0616%)
	FEM	62.95718	172.71836	339.95835	480.36575	891.55583
SS	NAM	26.85947 (0.0085%)	109.60386 (0.0119%)	239.57739 (0.0224%)	386.62265 (0.0346%)	659.12812 (0.0410%)
	FEM	26.86177	109.61694	239.63125	386.75668	659.39873

Note: The percentage differences between $\bar{\omega}_{jNAM}$ and $\bar{\omega}_{jFEM}$ shown in the parentheses ( ) were determined with the formula: $\varepsilon_j^* = (\bar{\omega}_{jFEM} - \bar{\omega}_{jNAM}) \times 100\% / \bar{\omega}_{jFEM}$

Table 6 The lowest five natural frequencies for the doubly-tapered beam carrying five translational springs with locations and magnitudes shown in Table 4 (Case 2)

Boundary conditions	Methods	Natural frequencies (rad/sec)				
		$\bar{\omega}_1$	$\bar{\omega}_2$	$\bar{\omega}_3$	$\bar{\omega}_4$	$\bar{\omega}_5$
FC	NAM	26.29514 (0.0124%)	109.02847 (0.0156%)	270.75305 (0.0272%)	511.67078 (0.0298%)	832.53629 (0.0302%)
	FEM	26.29841	109.04551	270.82695	511.82345	832.78851
CF	NAM	8.01201 (0.0229%)	73.58781 (0.0233%)	236.85090 (0.0244%)	477.61491 (0.0283%)	798.40294 (0.0324%)
	FEM	8.01385	73.60496	236.90878	477.75025	798.66244
SC	NAM	71.75531 (0.0144%)	212.92459 (0.0188%)	433.87894 (0.0226%)	734.72216 (0.0226%)	1115.58902 (0.0236%)
	FEM	71.76570	212.96469	433.97730	734.88810	1115.85300
CS	NAM	53.93133 (0.0117%)	196.27981 (0.0160%)	417.07681 (0.0159%)	717.83287 (0.0159%)	1098.65660 (0.0161%)
	FEM	53.93766	196.31121	417.14301	717.94694	1098.83335
CC	NAM	91.93714 (0.0078%)	251.79607 (0.0078%)	492.39517 (0.0079%)	813.03983 (0.0080%)	1213.80835 (0.0082%)
	FEM	91.94429	251.81572	492.43390	813.10483	1213.90843
SS	NAM	38.99935 (0.0013%)	162.28989 (0.0059%)	363.53401 (0.0067%)	644.50344 (0.0091%)	1005.43491 (0.0097%)
	FEM	38.99984	162.29947	363.55836	644.56219	1005.53216

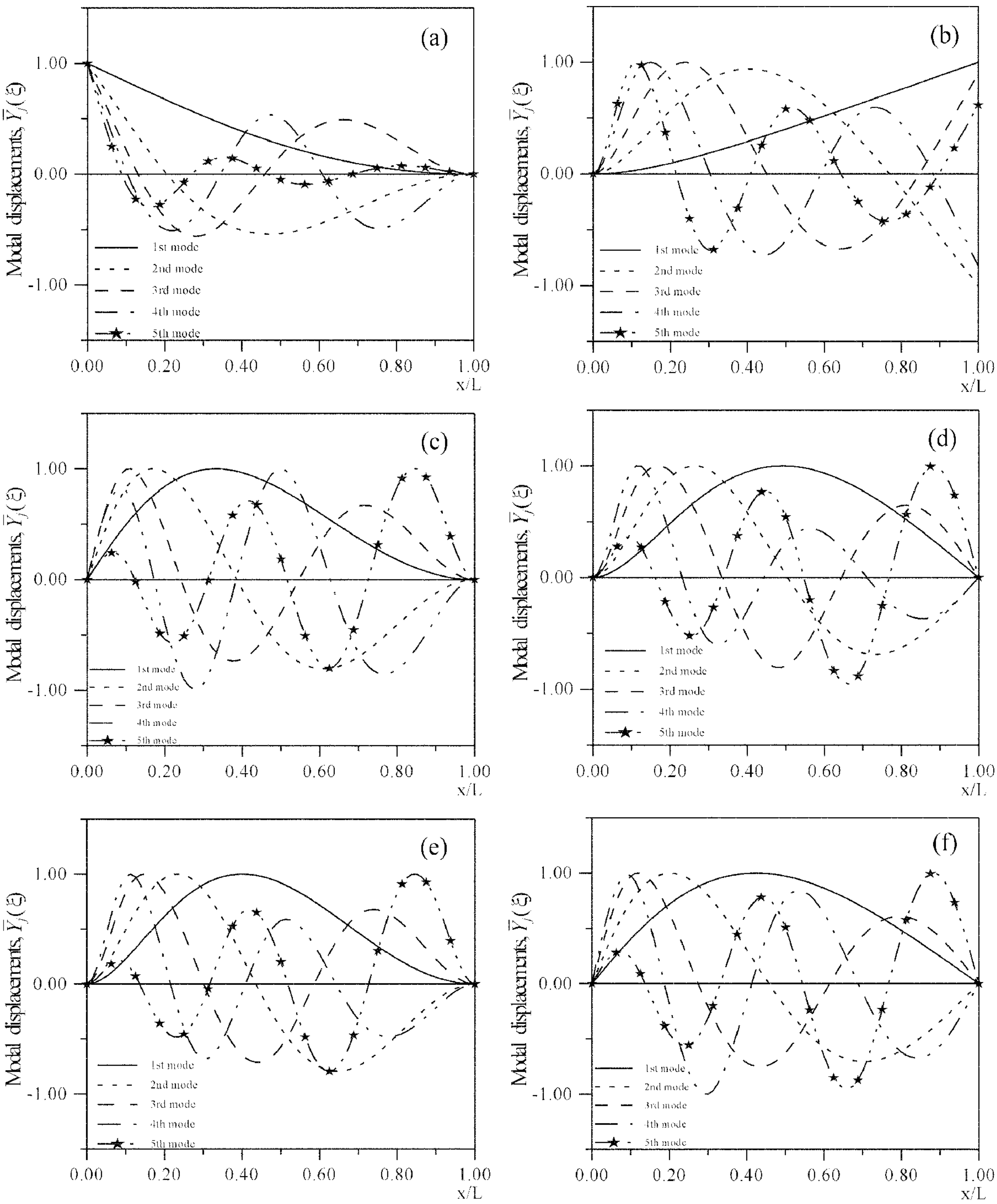

Fig. 4 The lowest five mode shapes $\overline{Y}_j(\xi)$ (j = 1~5) for the doubly-tapered beam carrying five point masses with locations and magnitudes shown in Table 4 for the support conditions: (a) FC, (b) CF, (c) SC, (d) CS, (e) CC and (f) SS

Table 7 The lowest five natural frequencies for the doubly-tapered beam carrying five rotational springs with locations and magnitudes shown in Table 4 (Case 3)

Boundary conditions	Methods	Natural frequencies (rad/sec)				
		$\bar{\omega}_1$	$\bar{\omega}_2$	$\bar{\omega}_3$	$\bar{\omega}_4$	$\bar{\omega}_5$
FC	NAM	28.57494 (0.0206%)	113.36598 (0.0296%)	275.08862 (0.0332%)	516.08580 (0.0461%)	835.99703 (0.0469%)
	FEM	28.58084	113.39965	275.18016	516.32394	836.39012
CF	NAM	9.92873 (0.0129%)	76.34653 (0.0218%)	239.57561 (0.0242%)	480.79005 (0.0406%)	800.93904 (0.0448%)
	FEM	9.93002	76.36314	239.63380	480.98562	801.29828
SC	NAM	73.51209 (0.0131%)	215.18391 (0.0133%)	436.01313 (0.0312%)	735.64242 (0.0332%)	1117.93677 (0.0339%)
	FEM	73.52172	215.21274	436.14948	735.88716	1118.31519
CS	NAM	55.44877 (0.0152%)	198.43105 (0.0158%)	419.82751 (0.0158%)	720.59389 (0.0158%)	1098.94536 (0.0162%)
	FEM	55.45725	198.46246	419.89382	720.70791	1099.12295
CC	NAM	93.25099 (0.0076%)	253.95781 (0.0077%)	495.19543 (0.0078%)	815.19702 (0.0080%)	1214.95692 (0.0082%)
	FEM	93.25809	253.97731	495.23398	815.26203	1215.05692
SS	NAM	41.05421 (0.0027%)	164.70974 (0.0113%)	365.89295 (0.0122%)	645.95905 (0.0242%)	1006.46270 (0.0290%)
	FEM	41.05532	164.72836	365.93775	646.11574	1006.75493

Table 8 The lowest five natural frequencies for the doubly-tapered beam carrying five point masses, five translational springs and five rotational springs with locations and magnitudes shown in Table 4 (Case 4)

Boundary conditions	Methods	Natural frequencies (rad/sec)				
		$\bar{\omega}_1$	$\bar{\omega}_2$	$\bar{\omega}_3$	$\bar{\omega}_4$	$\bar{\omega}_5$
FC	NAM	17.95168 (0.0155%)	76.56920 (0.0230%)	194.61172 (0.0341%)	387.01715 (0.0595%)	688.08834 (0.0630%)
	FEM	17.95447	76.58686	194.67814	387.24765	688.52217
CF	NAM	8.02218 (0.0194%)	54.51508 (0.0218%)	167.52606 (0.0217%)	338.80454 (0.0339%)	481.14907 (0.0343%)
	FEM	8.02374	54.52701	167.56256	338.91961	481.31423
SC	NAM	49.41539 (0.0150%)	144.42144 (0.0208%)	281.10500 (0.0223%)	435.36013 (0.0225%)	888.03352 (0.0415%)
	FEM	49.42281	144.45156	281.16784	435.45835	888.40263
CS	NAM	39.23242 (0.0187%)	136.44081 (0.0183%)	290.24124 (0.0243%)	450.23705 (0.0438%)	665.32369 (0.0515%)
	FEM	39.23978	136.46584	290.31181	450.43445	665.35801
CC	NAM	64.00580 (0.0104%)	174.17462 (0.0112%)	341.44197 (0.0240%)	480.54032 (0.0291%)	892.59772 (0.0392%)
	FEM	64.01249	174.19418	341.52403	480.68022	892.94784
SS	NAM	28.60715 (0.0036%)	111.27047 (0.0065%)	240.81870 (0.0068%)	387.07959 (0.0078%)	659.92196 (0.0095%)
	FEM	28.60818	111.27877	240.83519	387.11016	659.98481

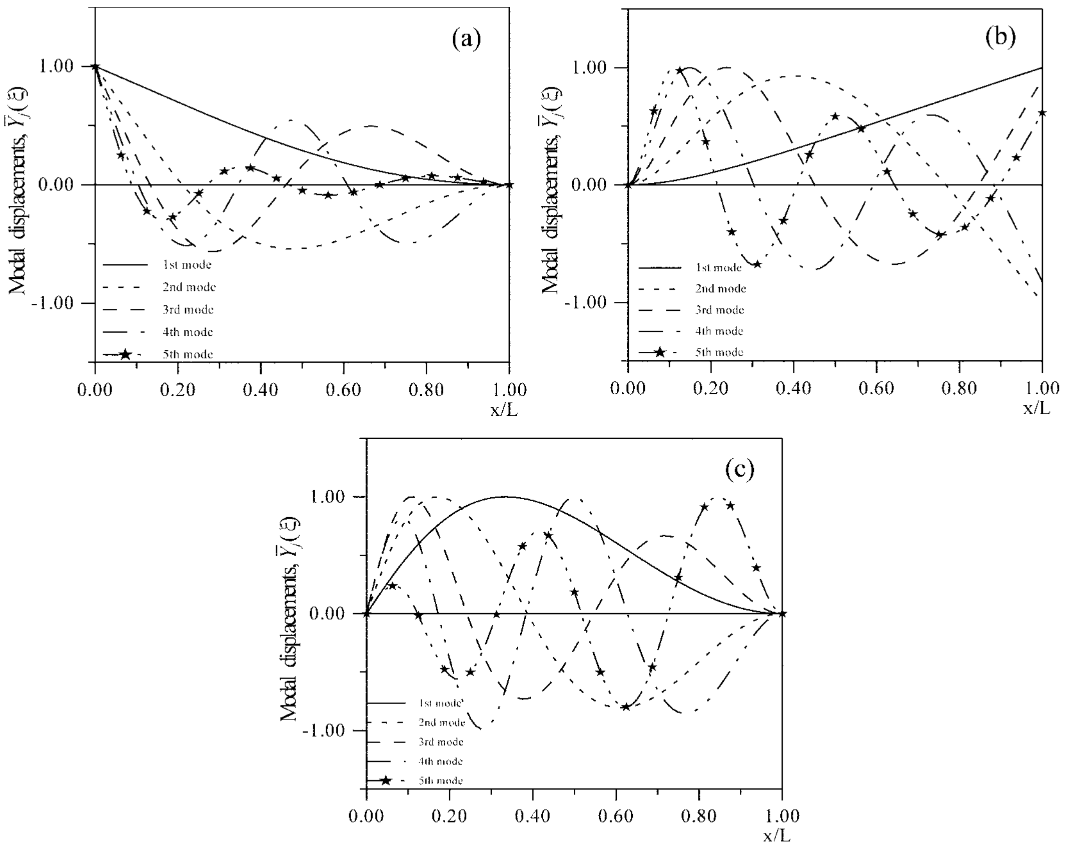

Fig. 5 The lowest five mode shapes $\overline{Y}_j(\xi)$ (j = 1~5) for the doubly-tapered beam carrying five point masses, five translational springs and five rotational springs with locations and magnitudes shown in Table 4 for the support conditions: (a) FC, (b) CF, (c) SC, (d) CS, (e) CC and (f) SS

8.4 Influence of magnitude and location of the single point mass m_c

If $m_c^* = m_c/m_b$, then the influence of location of the single point mass m_c with magnitudes $m_c^* = 1$, $m_c^* = 5$ and $m_c^* = 10$, respectively, on the lowest three natural frequencies of the constrained CF doubly-tapered beam were shown in Figs. 6(a) for the first frequency $\overline{\omega}_1$, 6(b) for the second one $\overline{\omega}_2$ and 6(c) for the third one $\overline{\omega}_3$. From Fig. 6(a) one sees that the first natural frequency ($\overline{\omega}_1$) of the CF beam decreases when the distance between the single point mass m_c and the left clamped end of the beam, x_c (or $\xi_c = x_c/L$, L is the beam length), increases; besides, at any specified location of the single point mass m_c(i.e., x_c = constant), the value of $\overline{\omega}_1$ decreases with increasing the magnitude of the single point mass. The last results are due to the fact that, for the first mode shape of the CF beam, the effective spring constant is given by $k_c = 3EI/x_c^3$ and the value of $\overline{\omega}_1$ is proportional to $\sqrt{k_c/m_c}$. From Figs. 6(b) and 6(c) one sees that, at any specified location of the single point mass m_c, the value of $\overline{\omega}_2$ (or $\overline{\omega}_3$) also decreases with increasing the magnitude of the single point mass m_c, but the influence of location of the single point mass on the second natural frequency $\overline{\omega}_2$ and the third one $\overline{\omega}_3$ is more complicated. From the second and third

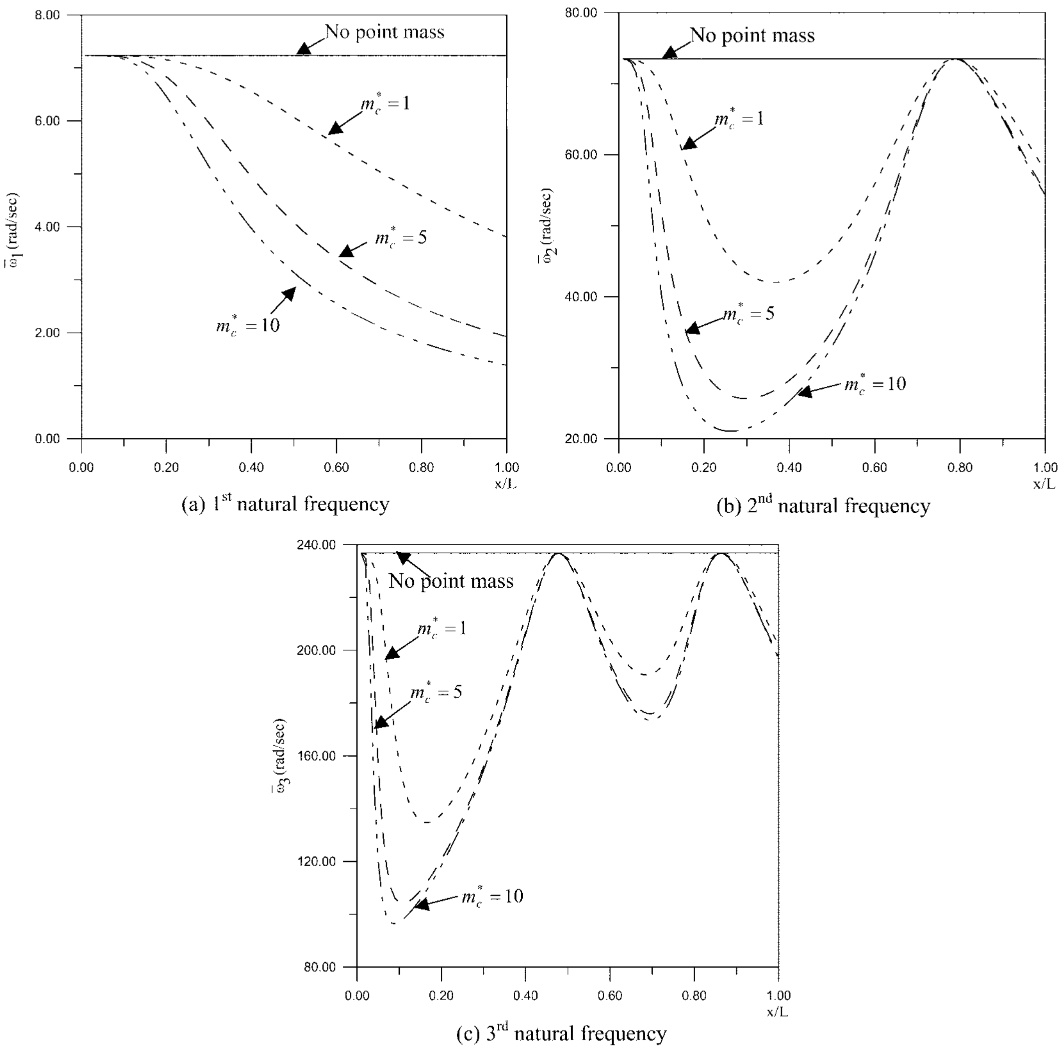

Fig. 6 Influence of magnitude and location of the single point mass on the lowest three natural frequencies of the CF doubly-tapered beam: (a) first frequency $\bar{\omega}_1$; (b) second frequency $\bar{\omega}_2$; (c) third frequency $\bar{\omega}_3$

mode shapes of the "unconstrained" CF tapered beam shown in Fig. 3(b) one sees that there exists one node at $x \approx 0.78L$ in the second mode shape and two nodes at $x \approx 0.47L$ and $0.86L$, respectively, in the second mode shape. This will be the reason why the second natural frequency ($\bar{\omega}_2$) of the constrained tapered beam for the case of $m_c^* = 1$ is equal to that with $m_c^* = 5$ or $m_c^* = 10$ when the point mass is located at $x_c \approx 0.78L$ (or $\xi_c = x_c/L \approx 0.78$) as one may see from Fig. 6(b). Similarly, when the point mass is located at node 1 with $x_{c1} \approx 0.47L$ or node 2 with $x_{c2} \approx 0.86L$, the influence of the magnitude of the point mass ($m_c^* = 1$, 5 or 10) on the third natural frequency ($\bar{\omega}_3$) of the constrained tapered beam is nil as shown in Fig. 6(c). It is noted that the horizontal solid lines in Figs. 6(a), 6(b) and 6(c) were used to indicate the first, second and third natural frequencies of the "unconstrained" CF tapered beam, respectively.

9. Conclusions

(1) For a doubly-tapered beam with various boundary conditions and carrying more than "two" concentrated elements, the exact natural frequencies and the corresponding mode shapes are easily determined with the numerical assembly method (NAM).

(2) The modal displacements near the left end of the "unconstrained" doubly-tapered SC, CS, CC, or SS beam are larger than those near the right end of the beam. This is a reasonable result, because the stiffness of the left end is much smaller than that of the right end for the doubly-tapered beam studied in this paper.

(3) The free vibration characteristics of a tapered beam are significantly influenced by the distributions and magnitudes of the concentrated attachments along the beam length.

(4) If the total number of nodes for the r-th mode shape is q and the distance between the point mass m_c and the left supporting end of the constrained beam is denoted by x_{ci}, then the influence of magnitude of the point mass on the corresponding natural frequency $\bar{\omega}_r$ is nil, when the point mass is located at $x = x_{ci}(i = 1{\sim}q)$ (i.e., located at any of the nodes).

References

Bathe, K.J. and Wilson, E.L. (1976), *Numerical Methods in Finite Element Analysis*, Prentice-Hall, Inc., Englewood Cliffs, N. J.

De Rosa, M.A. and Auciello, N.M. (1996), "Free vibrations of tapered beams with flexible ends", *Comput. Struct.*, **60**(2), 197-202.

Faires, J.D. and Burden, R.L. (1993), *Numerical Methods,* PWS Publishing Company, Boston, USA.

Gorman, Daniel I. (1975), *Free Vibration Analysis of Beams and Shafts*, John Wiley & Sons, Inc.

Gurgoze, M. (1984), "A note on the vibrations of restrained beam and rods with point masses", *J. Sound Vib.*, **96**, 461-468.

Gurgoze, M. (1998), "On the alternative formulations of the frequency equations of a Bernoulli-Euler beam to which several spring-mass systems are attached inspan", *J. Sound Vib.*, **217**(3), 585-595.

Hamdan, M.N. and Jubran, B.A. (1991) "Free and forced vibrations of a restrained uniform beam carrying an intermediate lumped mass and a rotary inertia", *J. Sound Vib.*, **150**(2), 203-216.

Karman, Theodore V. and Biot, Maurice A. (1940), *Mathematical Methods in Engineering,* New York: McGraw-Hill.

Laura, P.A.A., Maurizi, M.J. and Pombo, J.L. (1975), "A note on the dynamic analysis of an elastically restrained-free beam with a mass at the free end", *J. Sound Vib.*, **41**, 397-405.

Laura, P.A.A., Susemihl, E.A., Pombo, J.L., Luisoni, L.E. and Gelos, R. (1977), "On the dynamic behavior of structural elements carrying elastically mounted concentrated masses", *Applied Acoustic*, **10**, 121-145.

Laura, P.A.A., Filipich, C.P. and Cortinez, V.H. (1987), "Vibration of beams and plates carrying concentrated masses", *J. Sound Vib.*, **112**, 177-182.

Lee, T.W. (1976), "Transverse vibrations of a tapered beam carrying a concentrated mass", *J. Appl. Mech.*, Transactions of ASME, **43**(2), 366-367.

Li, Q.S. (2002), "Free vibration analysis of non-uniform beams with an arbitrary number of cracks and concentrated masses", *J. Sound Vib.*, **252**(3), 509-525.

Qiao, H., Li, Q.S. and Li, G.Q. (2002), "Vibratory characteristics of flexural non-uniform Euler-Bernoulli beams carrying an arbitrary number of spring-mass systems", *Int. J. Mech. Sci.*, **44**, 725-743.

Rossi, R.E., Laura, P.A.A., Avalos, D.R. and Larrondo, H. (1993), "Free vibration of Timoshenko beams carrying elastically mounted", *J. Sound Vib.*, **165**(2), 209-223.

Sankaran, G.V., Raju, K. Kanaka and Rao, G. Venkatesware (1975), "Vibrations frequencies of a tapered beam with one end and spring-hinged and carrying a mass at the other free end", *J. Appl. Mech.*, Transactions of ASME, **42**(3), 740-741.

Wu, J.S. and Lin, T.L. (1990), "Free vibration analysis of a uniform cantilever beam with point masses by an analytical-and-numerical-combined method", *J. Sound Vib.*, **136**, 201-213.
Wu, J.S. and Chou, H.M. (1998), "Free vibration analysis of a cantilever beam carrying any number of elastically mounted point masses with the analytical-and-numerical-combined method", *J. Sound Vib.*, **213**(2), 317-332.
Wu, J.S. and Chen, D.W. (2001), "Free vibration analysis of a Timoshenko beam carrying multiple spring-mass systems by using the numerical assembly technique", *Int. J. Num. Meth. Eng.*, **50**, 1039-1058.
Wu, J.S. and Chou, H.M. (1999), "A new approach for determining the natural frequencies and mode shapes of a uniform beam carrying any number of sprung masses", *J. Sound Vib.*, **220**(3), 451-468.

Appendix 1

For a non-uniform cantilever beam (CF) respectively carrying one and two concentrated elements, the "explicit" expressions for the overall coefficient matrices $[B]_{(1)}$ and $[B]_{(2)}$ were given by Eqs. (A1) and (A2), respectively.

$$[B]_{(1)} = \begin{array}{c} \begin{array}{cccccccc} \bar{C}_1 & \bar{C}_2 & \bar{C}_3 & \bar{C}_4 & \bar{C}_5 & \bar{C}_6 & \bar{C}_7 & \bar{C}_8 \end{array} \\ \left[\begin{array}{cccccccc} J_2(\beta) & Y_2(\beta) & I_2(\beta) & K_2(\beta) & 0 & 0 & 0 & 0 \\ J_3(\beta) & Y_3(\beta) & -I_3(\beta) & K_3(\beta) & 0 & 0 & 0 & 0 \\ J_2(\delta_1) & Y_2(\delta_1) & I_2(\delta_1) & K_2(\delta_1) & -J_2(\delta_1) & -Y_2(\delta_1) & -I_2(\delta_1) & -K_2(\delta_1) \\ J_3(\delta_1) & Y_3(\delta_1) & -I_3(\delta_1) & K_3(\delta_1) & -J_3(\delta_1) & -Y_3(\delta_1) & I_3(\delta_1) & -K_3(\delta_1) \\ \nabla_{11} & \nabla_{21} & \nabla_{31} & \nabla_{41} & -\nabla_{51} & -\nabla_{61} & -\nabla_{71} & -\nabla_{91} \\ \Delta_{11} & \Delta_{21} & \Delta_{31} & \Delta_{41} & -\Delta_{51} & -\Delta_{61} & -\Delta_{71} & -\Delta_{81} \\ 0 & 0 & 0 & 0 & J_4(\beta\sqrt{\alpha}) & Y_4(\beta\sqrt{\alpha}) & I_4(\beta\sqrt{\alpha}) & K_4(\beta\sqrt{\alpha}) \\ 0 & 0 & 0 & 0 & \varepsilon_1 & \varepsilon_2 & \varepsilon_3 & \varepsilon_4 \end{array}\right] \end{array} \begin{array}{c} \\ 1 \\ 2 \\ 3 \\ 4 \\ 5 \\ 6 \\ 7 \\ 8 \end{array} \quad \text{(A1)}$$

where

$$\nabla_{11} = \beta^2 J_4(\delta_1) - \frac{2k_{R1}^*}{(\alpha-1)}\beta\xi_1^{-7/2}J_3(\delta_1), \quad \nabla_{21} = \beta^2 Y_4(\delta_1) - \frac{2k_{R1}^*}{(\alpha-1)}\beta\xi_1^{-7/2}Y_3(\delta_1),$$

$$\nabla_{31} = \beta^2 I_4(\delta_1) + \frac{2k_{R1}^*}{(\alpha-1)}\beta\xi_1^{-7/2}I_3(\delta_1), \quad \nabla_{41} = \beta^2 K_4(\delta_1) - \frac{2k_{R1}^*}{(\alpha-1)}\beta\xi_1^{-7/2}K_3(\delta_1),$$

$$\nabla_{51} = \beta^2 J_4(\delta_1), \quad \nabla_{61} = \beta^2 Y_4(\delta_1), \quad \nabla_{71} = \beta^2 I_4(\delta_1), \quad \nabla_{81} = \beta^2 K_4(\delta_1),$$

$$\varepsilon_1 = [8J_4(\beta\sqrt{\alpha}) - \beta\alpha^{1/2}J_5(\beta\sqrt{\alpha})], \quad \varepsilon_2 = [8Y_4(\beta\sqrt{\alpha}) - \beta\alpha^{1/2}Y_5(\beta\sqrt{\alpha})],$$

$$\varepsilon_3 = [8I_4(\beta\sqrt{\alpha}) + \beta\alpha^{1/2}I_5(\beta\sqrt{\alpha})], \quad \varepsilon_4 = [8K_4(\beta\sqrt{\alpha}) - \beta\alpha^{1/2}K_5(\beta\sqrt{\alpha})]$$

$$\beta = 2L\Omega/(\alpha-1), \quad \Delta_{11} = 8\beta^2 J_4(\beta\sqrt{\xi_1}) - \beta^3\xi_1^{1/2}J_5(\beta\sqrt{\xi_1}) - 8\theta_1\xi_1^{-2}J_2(\beta\sqrt{\xi_1}),$$

$$\delta_1 = \beta\sqrt{\xi_1}, \quad \Delta_{21} = 8\beta^2 Y_4(\beta\sqrt{\xi_1}) - \beta^3\xi_1^{1/2}Y_5(\beta\sqrt{\xi_1}) - 8\theta_1\xi_1^{-2}Y_2(\beta\sqrt{\xi_1}),$$

$$\Delta_{31} = 8\beta^2 I_4(\beta\sqrt{\xi_1}) + \beta^3\xi_1^{1/2}I_5(\beta\sqrt{\xi_1}) - 8\theta_1\xi_1^{-2}I_2(\beta\sqrt{\xi_1}),$$

$$\Delta_{41} = 8\beta^2 K_4(\beta\sqrt{\xi_1}) - \beta^3 \xi_1^{1/2} K_5(\beta\sqrt{\xi_1}) - 8\theta_1 \xi_1^{-2} K_2(\beta\sqrt{\xi_1}),$$

$$\Delta_{51} = 8\beta^2 J_4(\beta\sqrt{\xi_1}) - \beta^3 \xi_1^{1/2} J_5(\beta\sqrt{\xi_1}), \quad \Delta_{61} = 8\beta^2 Y_4(\beta\sqrt{\xi_1}) - \beta^3 \xi_1^{1/2} Y_5(\beta\sqrt{\xi_1}),$$

$$\Delta_{71} = 8\beta^2 I_4(\beta\sqrt{\xi_1}) + \beta^3 \xi_1^{1/2} I_5(\beta\sqrt{\xi_1}), \quad \Delta_{81} = 8\beta^2 K_4(\beta\sqrt{\xi_1}) - \beta^3 \xi_1^{1/2} K_5(\beta\sqrt{\xi_1})$$

$$\theta_1 = \frac{k_{T1}^*}{(\alpha-1)^3} - \frac{m_{c1}^*\left[\frac{1}{3}(\alpha-1)^2 + \alpha\right](\Omega L)^4}{(\alpha-1)^3}$$

$$[B]_{(2)} = \begin{array}{c} \begin{array}{cccccccccccc} \overline{C}_1 & \overline{C}_2 & \overline{C}_3 & \overline{C}_4 & \overline{C}_5 & \overline{C}_6 & \overline{C}_7 & \overline{C}_8 & \overline{C}_9 & \overline{C}_{10} & \overline{C}_{11} & \overline{C}_{12} \end{array} \\ \left[\begin{array}{cccccccccccc}
J_2(\beta) & Y_2(\beta) & I_2(\beta) & K_2(\beta) & 0 & 0 & 0 & 0 & 0 & 0 & 0 & 0 \\
J_3(\beta) & Y_3(\beta) & -I_3(\beta) & K_3(\beta) & 0 & 0 & 0 & 0 & 0 & 0 & 0 & 0 \\
J_2(\delta_1) & Y_2(\delta_1) & I_2(\delta_1) & K_2(\delta_1) & -J_2(\delta_1) & -Y_2(\delta_1) & -I_2(\delta_1) & -K_2(\delta_1) & 0 & 0 & 0 & 0 \\
J_3(\delta_1) & Y_3(\delta_1) & -I_3(\delta_1) & K_3(\delta_1) & -J_3(\delta_1) & -Y_3(\delta_1) & I_3(\delta_1) & -K_3(\delta_1) & 0 & 0 & 0 & 0 \\
\nabla_{11} & \nabla_{21} & \nabla_{31} & \nabla_{41} & -\nabla_{51} & -\nabla_{61} & -\nabla_{71} & -\nabla_{81} & 0 & 0 & 0 & 0 \\
\Delta_{11} & \Delta_{21} & \Delta_{31} & \Delta_{41} & -\Delta_{51} & -\Delta_{61} & -\Delta_{71} & -\Delta_{81} & 0 & 0 & 0 & 0 \\
0 & 0 & 0 & 0 & J_2(\delta_2) & Y_2(\delta_2) & I_2(\delta_2) & K_2(\delta_2) & -J_2(\delta_2) & -Y_2(\delta_2) & -I_2(\delta_2) & -K_2(\delta_2) \\
0 & 0 & 0 & 0 & J_3(\delta_2) & Y_3(\delta_2) & -I_3(\delta_2) & K_3(\delta_2) & -J_3(\delta_2) & -Y_3(\delta_2) & I_3(\delta_2) & -K_3(\delta_2) \\
0 & 0 & 0 & 0 & \nabla_{12} & \nabla_{22} & \nabla_{32} & \nabla_{42} & -\nabla_{52} & -\nabla_{62} & -\nabla_{72} & -\nabla_{82} \\
0 & 0 & 0 & 0 & \Delta_{12} & \Delta_{22} & \Delta_{32} & \Delta_{42} & -\Delta_{52} & -\Delta_{62} & -\Delta_{72} & -\Delta_{82} \\
0 & 0 & 0 & 0 & 0 & 0 & 0 & 0 & J_4(\beta\sqrt{\alpha}) & Y_4(\beta\sqrt{\alpha}) & I_4(\beta\sqrt{\alpha}) & K_4(\beta\sqrt{\alpha}) \\
0 & 0 & 0 & 0 & 0 & 0 & 0 & 0 & \varepsilon_1 & \varepsilon_2 & \varepsilon_3 & \varepsilon_4
\end{array}\right] \end{array} \begin{array}{c} \\ 1 \\ 2 \\ 3 \\ 4 \\ 5 \\ 6 \\ 7 \\ 8 \\ 9 \\ 10 \\ 11 \\ 12 \end{array} \tag{A2}$$

where

$$\nabla_{1\nu} = \beta^2 J_4(\delta_\nu) - \frac{2k_{R\nu}^*}{(\alpha-1)} \beta \xi_\nu^{-7/2} J_3(\delta_\nu), \quad \nabla_{2\nu} = \beta^2 Y_4(\delta_\nu) - \frac{2k_{R\nu}^*}{(\alpha-1)} \beta \xi_\nu^{-7/2} Y_3(\delta_\nu),$$

$$\nabla_{3\nu} = \beta^2 I_4(\delta_\nu) + \frac{2k_{R\nu}^*}{(\alpha-1)} \beta \xi_\nu^{-7/2} I_3(\delta_\nu), \quad \nabla_{4\nu} = \beta^2 K_4(\delta_\nu) - \frac{2k_{R\nu}^*}{(\alpha-1)} \beta \xi_\nu^{-7/2} K_3(\delta_\nu),$$

$$\nabla_{5\nu} = \beta^2 J_4(\delta_\nu), \quad \nabla_{6\nu} = \beta^2 Y_4(\delta_\nu), \quad \nabla_{7\nu} = \beta^2 I_4(\delta_\nu), \quad \nabla_{8\nu} = \beta^2 K_4(\delta_\nu), \quad \beta = 2L\Omega/(\alpha-1),$$

$$\Delta_{1\nu} = 8\beta^2 J_4(\beta\sqrt{\xi_\nu}) - \beta^3\xi_\nu^{1/2}J_5(\beta\sqrt{\xi_\nu}) - 8\theta_\nu\xi_\nu^{-2}J_2(\beta\sqrt{\xi_\nu}), \quad \delta_\nu = \beta\sqrt{\xi_\nu},$$

$$\Delta_{2\nu} = 8\beta^2 Y_4(\beta\sqrt{\xi_\nu}) - \beta^3\xi_\nu^{1/2}Y_5(\beta\sqrt{\xi_\nu}) - 8\theta_\nu\xi_\nu^{-2}Y_2(\beta\sqrt{\xi_\nu}),$$

$$\Delta_{3\nu} = 8\beta^2 I_4(\beta\sqrt{\xi_\nu}) + \beta^3\xi_\nu^{1/2}I_5(\beta\sqrt{\xi_\nu}) - 8\theta_\nu\xi_\nu^{-2}I_2(\beta\sqrt{\xi_\nu}),$$

$$\Delta_{4\nu} = 8\beta^2 K_4(\beta\sqrt{\xi_\nu}) - \beta^3\xi_\nu^{1/2}K_5(\beta\sqrt{\xi_\nu}) - 8\theta_\nu\xi_\nu^{-2}K_2(\beta\sqrt{\xi_\nu}),$$

$$\Delta_{5\nu} = 8\beta^2 J_4(\beta\sqrt{\xi_\nu}) - \beta^3\xi_\nu^{1/2}J_5(\beta\sqrt{\xi_\nu}), \quad \Delta_{6\nu} = 8\beta^2 Y_4(\beta\sqrt{\xi_\nu}) - \beta^3\xi_\nu^{1/2}Y_5(\beta\sqrt{\xi_\nu}),$$

$$\Delta_{7\nu} = 8\beta^2 I_4(\beta\sqrt{\xi_\nu}) + \beta^3\xi_\nu^{1/2}I_5(\beta\sqrt{\xi_\nu}), \quad \Delta_{8\nu} = 8\beta^2 K_4(\beta\sqrt{\xi_\nu}) - \beta^3\xi_\nu^{1/2}K_5(\beta\sqrt{\xi_\nu}),$$

$$\varepsilon_1 = [8J_4(\beta\sqrt{\alpha}) - \beta\alpha^{1/2}J_5(\beta\sqrt{\alpha})], \quad \varepsilon_2 = [8Y_4(\beta\sqrt{\alpha}) - \beta\alpha^{1/2}Y_5(\beta\sqrt{\alpha})],$$

$$\varepsilon_3 = [8I_4(\beta\sqrt{\alpha}) + \beta\alpha^{1/2}I_5(\beta\sqrt{\alpha})], \quad \varepsilon_4 = [8K_4(\beta\sqrt{\alpha}) - \beta\alpha^{1/2}K_5(\beta\sqrt{\alpha})],$$

$$\theta_\nu = \frac{k_{T\nu}^*}{(\alpha-1)^3} - \frac{m_{c\nu}^*\left[\frac{1}{3}(\alpha-1)^2 + \alpha\right](\Omega L)^4}{(\alpha-1)^3} (\nu = 1, 2)$$

Appendix 2

The coefficient matrices for the "left" end of the beam, $[B_L]$, and those for the "right" end of the beam, $[B_R]$, with the FC, SC, CS, CC and SS boundary conditions were given below.

(1) Free-clamped beam

$$[B_R] = \begin{array}{c} \begin{array}{cccc} 1 & 2 & 3 & 4 \end{array} \\ \begin{bmatrix} J_4(\beta) & Y_4(\beta) & I_4(\beta) & K_4(\beta) \\ 8J_4(\beta) - \beta J_5(\beta) & 8Y_4(\beta) - \beta Y_5(\beta) & 8I_4(\beta) + \beta I_5(\beta) & 8K_4(\beta) - \beta K_5(\beta) \end{bmatrix} \end{array} \begin{array}{c} \\ 1 \\ 2 \end{array} \tag{A3}$$

$$[B_L] = \begin{array}{c} \begin{array}{cccc} 4n+1 & 4n+2 & 4n+3 & 4n+4 \end{array} \\ \begin{bmatrix} J_2(\beta\sqrt{\alpha}) & Y_2(\beta\sqrt{\alpha}) & I_2(\beta\sqrt{\alpha}) & K_2(\beta\sqrt{\alpha}) \\ J_3(\beta\sqrt{\alpha}) & Y_3(\beta\sqrt{\alpha}) & -I_3(\beta\sqrt{\alpha}) & K_3(\beta\sqrt{\alpha}) \end{bmatrix} \end{array} \begin{array}{c} \\ p-1 \\ p \end{array} \tag{A4}$$

(2) Simply supported-clamped beam

$$[B_R] = \begin{array}{c} \begin{array}{cccc} 1 & 2 & 3 & 4 \end{array} \\ \begin{bmatrix} J_2(\beta) & Y_2(\beta) & I_2(\beta) & K_2(\beta) \\ J_4(\beta) & Y_4(\beta) & I_4(\beta) & K_4(\beta) \end{bmatrix} \end{array} \begin{array}{c} \\ 1 \\ 2 \end{array} \tag{A5}$$

$$[B_L] = \begin{array}{c} \begin{array}{cccc} 4n+1 & 4n+2 & 4n+3 & 4n+4 \end{array} \\ \begin{bmatrix} J_2(\beta\sqrt{\alpha}) & Y_2(\beta\sqrt{\alpha}) & I_2(\beta\sqrt{\alpha}) & K_2(\beta\sqrt{\alpha}) \\ J_3(\beta\sqrt{\alpha}) & Y_3(\beta\sqrt{\alpha}) & -I_3(\beta\sqrt{\alpha}) & K_3(\beta\sqrt{\alpha}) \end{bmatrix} \end{array} \begin{array}{c} \\ p-1 \\ p \end{array} \tag{A6}$$

(3) Clamped-simply supported

$$[B_R] = \begin{array}{c} \begin{array}{cccc} 1 & 2 & 3 & 4 \end{array} \\ \begin{bmatrix} J_2(\beta) & Y_2(\beta) & I_2(\beta) & K_2(\beta) \\ J_3(\beta) & Y_3(\beta) & -I_3(\beta) & K_3(\beta) \end{bmatrix} \end{array} \begin{array}{c} \\ 1 \\ 2 \end{array} \tag{A7}$$

$$[B_L] = \begin{array}{c c} 4n+1 \quad\quad 4n+2 \quad\quad 4n+3 \quad\quad 4n+4 & \\ \begin{bmatrix} J_2(\beta\sqrt{\alpha}) & Y_2(\beta\sqrt{\alpha}) & I_2(\beta\sqrt{\alpha}) & K_2(\beta\sqrt{\alpha}) \\ J_4(\beta\sqrt{\alpha}) & Y_4(\beta\sqrt{\alpha}) & I_4(\beta\sqrt{\alpha}) & K_4(\beta\sqrt{\alpha}) \end{bmatrix} & \begin{array}{c} p-1 \\ p \end{array} \end{array} \tag{A8}$$

(4) Clamped-clamped

$$[B_R] = \begin{array}{c c} 1 \quad\quad 2 \quad\quad 3 \quad\quad 4 & \\ \begin{bmatrix} J_2(\beta) & Y_2(\beta) & I_2(\beta) & K_2(\beta) \\ J_3(\beta) & Y_3(\beta) & -I_3(\beta) & K_3(\beta) \end{bmatrix} & \begin{array}{c} 1 \\ 2 \end{array} \end{array} \tag{A9}$$

$$[B_L] = \begin{array}{c c} 4n+1 \quad\quad 4n+2 \quad\quad 4n+3 \quad\quad 4n+4 & \\ \begin{bmatrix} J_2(\beta\sqrt{\alpha}) & Y_2(\beta\sqrt{\alpha}) & I_2(\beta\sqrt{\alpha}) & K_2(\beta\sqrt{\alpha}) \\ J_3(\beta\sqrt{\alpha}) & Y_3(\beta\sqrt{\alpha}) & -I_3(\beta\sqrt{\alpha}) & K_3(\beta\sqrt{\alpha}) \end{bmatrix} & \begin{array}{c} p-1 \\ p \end{array} \end{array} \tag{A10}$$

(5) Simply supported-simply supported beam

$$[B_R] = \begin{array}{c c} 1 \quad\quad 2 \quad\quad 3 \quad\quad 4 & \\ \begin{bmatrix} J_2(\beta) & Y_2(\beta) & I_2(\beta) & K_2(\beta) \\ J_4(\beta) & Y_4(\beta) & I_4(\beta) & K_4(\beta) \end{bmatrix} & \begin{array}{c} 1 \\ 2 \end{array} \end{array} \tag{A11}$$

$$[B_L] = \begin{array}{c c} 4n+1 \quad\quad 4n+2 \quad\quad 4n+3 \quad\quad 4n+4 & \\ \begin{bmatrix} J_2(\beta\sqrt{\alpha}) & Y_2(\beta\sqrt{\alpha}) & I_2(\beta\sqrt{\alpha}) & K_2(\beta\sqrt{\alpha}) \\ J_4(\beta\sqrt{\alpha}) & Y_4(\beta\sqrt{\alpha}) & I_4(\beta\sqrt{\alpha}) & K_4(\beta\sqrt{\alpha}) \end{bmatrix} & \begin{array}{c} p-1 \\ p \end{array} \end{array} \tag{A12}$$